Macromolecules

Article

pubs.acs.org/Macromolecules

Complex Interactions with the Surroundings Dictate a Tagged Chain's Dynamics in Unentangled Polymer Melts

Debabrata Panja,*[,†] Gerard T. Barkema,[‡,§] and Robin C. Ball[∥]

[†]Institute of Physics, Universiteit van Amsterdam, Science Park 904, Postbus 94485, 1090 GL Amsterdam, The Netherlands

[‡]Institute for Theoretical Physics, Universiteit Utrecht, Leuvenlaan 4, 3584 CE Utrecht, The Netherlands

[§]Instituut-Lorentz, Universiteit Leiden, Niels Bohrweg 2, 2333 CA, Leiden, The Netherlands

[∥]Department of Physics, University of Warwick, Coventry CV4 7AL, U.K.

ABSTRACT: For more than half a century the theoretical landscape for single chain dynamics for dense polymeric solutions and melts below the entanglement threshold has been dominated by the Rouse model for independent phantom chains, supported by ideas of hydrodynamic screening. There exists, however, a large body of literature from experiments, Monte Carlo, and molecular dynamics simulations on the deviations from the Rouse behavior for unentangled homopolymer melts, showcased mostly in the subdiffusive behavior of center-of-mass of tagged chains at intermediate times, with the subdiffusion exponent reported in the range 0.75−0.85. The influence of the surrounding chains of length N_s on the motion of a single tagged chain of length N is a key test, by which, through high-precision numerical simulation of unentangled melts, we show that the Rouse model fails. Our central results are that at intermediate times the tagged chain's center-of-mass moves subdiffusively, $\langle \Delta r^2_{cm} \rangle \propto t^\alpha$ with subdiffusion exponent $\alpha = 0.87 \pm 0.03$ as opposed to $\alpha_{Rouse} = 1$, and that its crossover time to Fickian behavior is directly controlled by the relaxation time of the surrounding chains when the latter are shorter. The terminal relaxation time for the tagged chain and the long time diffusion coefficient are then sensitive to N_s. Both measured exponent flow, that is plots of $d\alpha(t)/d \ln (t)$ vs $\alpha(t)$ where $\alpha(t)$ is the effective exponent between $\langle \Delta r^2_{cm} \rangle$ and t, and successful blob scaling arguments support the anomalous value of α as a true exponent. We find the same exponent in the scaling of Rouse mode amplitude correlation functions and directly related exponent for the monomeric diffusion. We show that the consequences of these results on the dynamics of a tagged monomer and the chain's segmental orientation autocorrelation function agree very well with rheological measurements and NMR relaxometry experiments. We reflect back on a history of related experimental anomalies and discuss how a new theory might be developed.

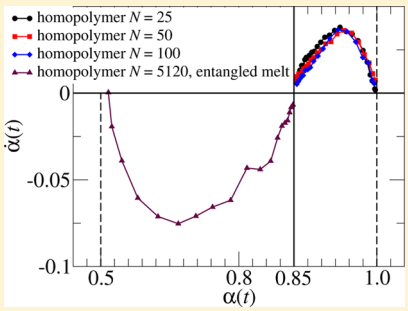

I. INTRODUCTION

Unlike a single chain in isolation, a tagged chain in a dense polymer system has to interact with the surrounding chains. Beyond the scale of the "entanglement length" $\mathcal{N}_e$, which is typically at least of order 100 backbone units even for a melt, it is widely recognized that topological constraints dramatically change the scaling of relaxation times for $N > \mathcal{N}_c \simeq 3\mathcal{N}_e$.

This paper concerns the subentangled regime, where we study the dynamics of tagged chains of length N in a surrounding matrix of chains of length N_s where $N_s < \mathcal{N}_e$ using Monte Carlo simulations, corresponding to both hydrodynamic and static screening holding true, for which one expects the Rouse model to be valid. Conventional expectation would be that the Rouse model should prevail, with the chains not just statically screened to Gaussian spatial statistics, which is well-established,[1] but also strongly hydrodynamically screened so that the motion of a chain is dominated by friction with respect to its immediate (monomeric) surroundings. The latter is characterized by the "monomeric friction factor", and its dominance leads to Rouse dynamics,[2] with the chain's center-of-mass (cm) moving diffusively at all times, with diffusion coefficient $D_{Rouse} \propto 1/N$. This should be the case until the hydrodynamic screening breaks down at $N \propto N_s^2$.[3] However, there exists a significant literature—experiments, MC (Monte Carlo) and MD (molecular dynamics) simulations on homopolymer melts (i.e., $N = N_s$)—that have found significant deviations from the expected Rouse behavior in the subentangled regime.[4−10] Most of the works have concentrated on the subdiffusive behavior of the cm of a tagged chain, with subdiffusion exponent α reported in the range 0.75−0.85, although (Rouse) mode autocorrelation functions have also been reported to decay in time as stretched exponentials with exponents in the same numerical range.[5,8−10]

Figure 1 shows the mean-square displacement (msd) of the cm for homopolymer melts: neutron spin echo (NSE) experiments with unentangled polybutadiene (PB) and polyethylene (PE), chemically realistic MD simulations, MC simulations with bond fluctuation model, and MD simulations with a bead−spring model. The cm msd is seen to increase as t^α with $\alpha \approx 0.81$ for about 3 decades in time.

Received: December 15, 2014
Revised: February 9, 2015
Published: February 20, 2015

DOI: 10.1021/ma502523p
Macromolecules 2015, 48, 1442−1453

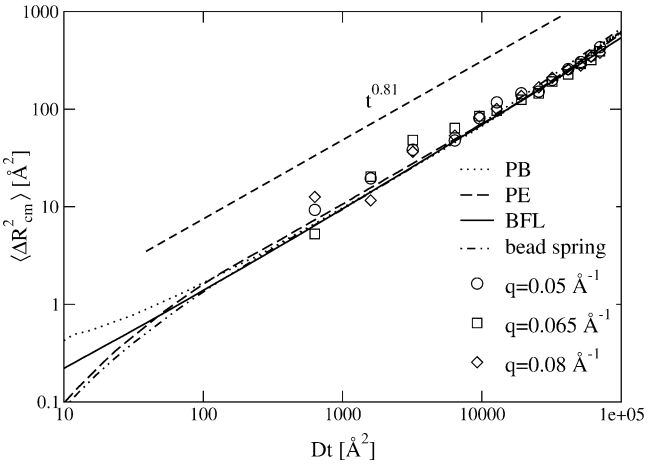

Figure 1. Center-of-mass displacement of tagged melt chains for different models in the unentangled regime. Chemically realistic MD simulations of PB (···) and PE (- - -), MC simulations of the bond-fluctuation model (—), and MD simulations of a bead−spring model (-·-·-). The symbols are obtained from neutron spin-echo (NSE) experiments (see ref 8 for details). Reproduced with permission from ref 8. Copyright 2004 IoP Publishing Ltd.

The subdiffusive dynamics of the cm msd of the tagged chain is a violation of the Rouse model for unentangled melts, at least if it is truly a power law, and it has a long history in simulation and theory. For the *measured* subdiffusion exponent, Schaffer[4] has reported 0.8 [bond fluctuation model (BFM)], Padding and Briels[6] have reported 0.8 [a coarse-grained molecular dynamics (MD) model], Paul and Smith[8] reported 0.81 ± 0.02 [experiments, Monte Carlo (MC) and MD simulations], Paul et al.[5,9] have reported 0.8 and 0.83, respectively (MD simulations), Pérez-Aparicio et al.[10] have reported 0.8−0.85 (experiments and MD simulations), and Wittmer et al.[7] have reported 0.8 (BFM). Note that these values all show a spread of approximately 5% within which our value falls. Schaffer further noticed that it makes a difference in the value of α when the chains in a melt are allowed to cross each other, an observation also made by Padding and Briels. On the theoretical side, on the basis of a mode-coupling approach, Schweizer proposed a "renormalized Rouse theory"[11] in which the tagged chain moves in an effective medium of the other polymers, where the density fluctuations of the medium give at first iteration $\alpha = 3/4$; however, when carried through to next order, the "twice renormalized Rouse theory"[12] reverted to $\alpha = 1$. Guenza generalized Schweizer's original approach to include explicit cross-chain interactions[13] leading to numerical fit with measured cm msd from simulations[14] and spin-echo experiments[15] without suggestion of a power law. More recently, Farago et al. argued (a) that the density fluctuation effects considered by Schweizer is only a subdominant effect,[16] and further (b) using a mode-coupling approach to address viscoelastic hydrodynamics of melts, they suggested that the observed subdiffusive regime of the cm motion is characterized by a simple (additive) crossover from $\alpha = 3/4$ to $\alpha = 1$.[17] In other words, Farago et al.[16,17] claim that $\alpha \simeq 0.8-0.85$ reported extensively in the literature is an effective exponent and further that the details differ between momentum-conserving and non-momentum-conserving systems (the works by Farago et al. are preluded by the simulation study by Wittmer et al.,[7] to which we will return later in the paper).

Relatively few real experiments have explored molecular weight dependence of the tagged chain's diffusion coefficient for $N \neq N_s$ for unentangled melts: dyed and photobleached poly(propylene oxide) chains in poly(propylene oxide) melt matrices[18,19] and deuterated polystyrene chains in undeuterated polystyrene matrices.[20] These experiments roughly agree that $D \sim N^{-0.6}N_s^{-1}$ for $N \gg N_s$, corresponding to both static and hydrodynamic screening breaking down in favor of swollen chains exhibiting Stokes diffusion $D_{\mathrm{Stokes}} \propto [\eta(N_s)R(N)]^{-1}$ in a medium governed by the matrix viscosity $\eta(N_s) \sim N_s$, so they are not suitable for a test of the Rouse model.

In this paper we expose the role of the surroundings of the tagged chain by studying the separate dependence on N_s and N for unentangled melts. We achieve this by comprehensively connecting the intermediate time dynamics of the system to its long-time dynamics. We find that the deviations from the Rouse behavior for the tagged chain is directly controlled by the length of the matrix chains N_s, thereby demonstrating the importance of the complex interactions between the tagged and the matrix chains. We find that cm subdiffusion exponent for the tagged chain and other measurements are all consistent with $\alpha = 0.87 \pm 0.03$, in excellent agreement with the values in the existing literature.

We also report the same exponent in mode amplitude correlation functions, which allows us to extract the deviations from the Rouse behavior for the dynamics of a tagged monomer and the chain's segmental orientation autocorrelation function.[21] Our prediction and numerical observations for these two quantities agree well with rheological measurements[22] and NMR relaxometry experimental data,[23−26] respectively.

The simulation details and the chosen system parameters are described in the section II. At the density we consider, the entanglement length $\mathcal{N}_e$ is at least 200. Our systems have exactly one tagged chain in a box of side considerably greater than its radius, so the tagged chains are strictly dilute but in a polymeric solvent. In this situation, the degree of entanglement length for our tagged chains is then dictated by $\mathcal{N} = \mathrm{Min}[N,N_s]$, and in order to maintain a safe distance from entanglement, we keep $\mathcal{N} \leq 100$. The high value of $\mathcal{N}_e$ arises because multiple occupancy of the same lattice site by the monomers belonging to the same chain is allowed: at our working density 0.95 approximately 45% of the sites typically remain empty, so $\mathcal{N}_e$ is elevated both by dilution and by near double count of occupied sites (see section II).

The paper is organized as follows. In section II we describe our model. In section III we present our results, and in section IV we discuss agreements of our key results with experimental data. The paper is concluded in section V with our preliminary thoughts on how a new theory might be formulated.

II. METHODS

Our simulations have been performed with the lattice polymer model described in ref 27. This model combines high computational efficiency with realistic polymer dynamics. Polymers consist of a string of monomers, and monomers adjacent in the string are located either in the same, or in neighboring sites of a face center cubic lattice in three dimensions. Polymer chain contours are self- and mutually avoiding; multiple occupation of lattice sites is not allowed, except for a sequential string of monomers belonging to the same chain. The chains move through a sequence of random single-monomer hops to neighboring lattice sites. These hops can be along the contour of the chain, thus explicitly providing reptation dynamics. They can also change the contour "sideways", providing Rouse dynamics. A two-dimensional version of our model is illustrated in Figure 2. The

DOI: 10.1021/ma502523p
Macromolecules 2015, 48, 1442−1453

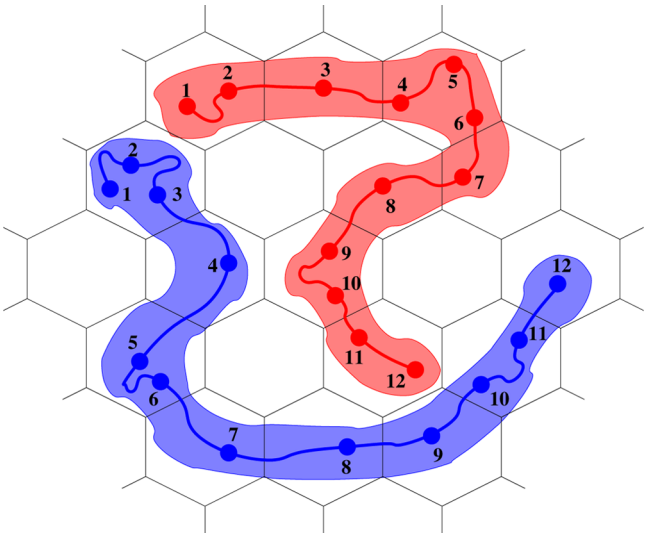

Figure 2. Illustration of the two-dimensional version of the lattice polymer model. Polymer chains are shown by darker colors and their contours in lighter colors. In the upper chain, interior monomers 2, 4, 6, 9, 10, and 11 can either move along the contour, or move sideways; monomer 7 can join either 6 or 8; the end monomers 1 and 12 can move to any empty nearest-neighbor site. In the lower chain, interior monomers 3, 5, 6, 10, and 11 can either move along the contour or move sideways; monomer 1 can move to any empty nearest-neighbor site, and monomer 12 can join its neighbor 11. In this configuration, because of the self- and mutually avoiding property of the chains, all other monomers cannot make a move. Statistically once per unit of time, each monomer attempts to move up and down along the contour, as well as sideways.

individual moves maintain detailed balance at all times. The time scale is set such that on average per unit of time each monomer attempts to move once along the contour and once sideways stretching or contracting the backbone. Lattice models introduce frictional forces of order unity per monomer, resulting in Rouse dynamics for single chains. Indeed, our model has been thoroughly checked for reproducing Rouse dynamics for single isolated chains, including the fluctuation−dissipation theorem for tagged monomeric motion.[28]

Our model is thus similar to the bond fluctuation model (BFM),[29] with the important difference that ergodicity problems and jamming at high monomeric densities are avoided by explicit reptation moves. Our model has been used by ourselves[28,30−36] and several other groups.[37,38] In our own research we have used it to simulate the diffusion and exchange of polymers in an equilibrated layer of adsorbed polymers,[30] the dynamics of self-avoiding Rouse polymers,[28] polymer translocation under a variety of circumstances,[31−34] dynamics of polymer adsorption,[35] and recently the dynamics of entangled melts (in excellent agreement with field-cycling NMR experiments[36]). From these studies we are not aware of any lattice artifacts of our model.

In detail, our simulations proceed as follows. All our simulations are performed with a lattice of 40^3 sites with periodic boundary conditions in all three directions. Initially, crumpled-up chains are placed on randomly chosen lattice sites, with one (tagged) chain of length N while the matrix chains are of length N_s. [Of course, for homopolymer melts ($N = N_s$) any chain can be treated as a tagged chain, which contributes greatly for statistics of our data.] The system is then brought to equilibrium by letting it evolve over some time $\tau_{eq}(N,N_s)$. In the main text, the terminal relaxation time of the chains of length N_s (N) is denoted by $\tau_t(N_s)$ ($\tau_t(N)$); we have chosen the equilibration time $\tau_{eq}(N,N_s) > 10\ \mathrm{Max}[\tau_t(N_s), \tau_t(N)]$. In all of our simulations the overall monomer density of the matrix chains is kept fixed at 0.95. After equilibration, overall, approximately 45% of the sites typically remain empty, due to the possibility that adjacent monomers belonging to the same chain can occupy the same lattice site.

At overall monomer density unity, from measurements of the rheological stress relaxation modulus $G(t)$, we have determined the entanglement length $\mathcal{N}_e$ to be 200 ± 20.[36] This means that the entanglement length $\mathcal{N}_e$ for the present study, performed at overall monomer density 0.95, should be at least 200. We simulate with only one tagged chain in a box of side considerably greater than its radius, so the tagged chains are strictly dilute but in a polymeric solvent. The degree of entanglement for our tagged chains is then dictated by $\mathcal{N} = \mathrm{Min}[N,N_s]$, and in order to maintain a safe distance from entanglement, we keep $\mathcal{N} \leq 100$.

After equilibration, a sequence of 200 000 snapshots of the tagged chain is stored, separated by a regular time interval. In the first set, the "long time set", the time difference between consecutive snapshots of the time series is chosen to be somewhere between 50 and 1000 units of time. In the second set, the "short time set", the time difference between consecutive snapshots of the time series is chosen to be somewhere between 5 and 20 units of time. Unless $N = N_s$, each simulation is carried out at least 32 independent times in order to improve statistics. The long- and short-time data for the relevant variable for the tagged chain are respectively averaged over these independent simulations and then merged together to produce the graphs in this paper.

III. RESULTS

A. Case $N \geq N_s$. *1. Mean-Square Displacement for the Tagged Chain's Center of Mass.* First we consider the msd of the cm of the tagged chain.

In Figure 3a−d we present the cm msd data for our model, showing that the crossover of its subdiffusive to diffusive behavior is directly controlled by the length of the surrounding chains. In detail, Figure 3a shows that the effective exponent of the cm msd, i.e., $\ln(\langle \Delta r^2_{cm}(t)\rangle)$ data numerically differentiated with respect to $\ln(t)$, for the tagged chain for all (N, N_s) combinations. All the effective exponents exhibit a crossover from a value approximately 0.85 at short times to unity at long times.

Figure 3b shows that it is fundamentally N_s which controls the crossover, with the dependence on N being removed when time is scaled by the simple scaling function $f(N/N_s)$, which depends only on the ratio N/N_s and not on the two chain lengths separately. The values of this scaling function are given in Table 1. Importantly, $f(x)$ appears to be saturating for large x rather than growing as a power of x. Note that if for example the crossover time were really set by $\tau^*(N)$, then scaling time by f could only remove the N dependence if $f(x) \propto x^{2/\alpha}$, which is far from the case. For the exponent crossover in homopolymers ($N/N_s = 1$) there is only the pure dependence on N_s, and Figure 3c shows this can be very accurately removed by scaling time by a characteristic time scale for the chain conformation. We measured this independently in terms of the relaxation time scale $\tau^*(N_s)$ for the end-to-end vector correlation of a tagged chain in the homopolymer samples. The measurement quality for $\tau^*(N_s)$ and values resulting are shown in Figure 4a.

Combining all the above, Figure 3d shows that all the exponent crossover data for different combinations of $N \geq N_s$ fall on a single universal master curve when we scale time both by $f(N/N_s)$ and by the fundamental time scale of the solvent chains captured by $\tau^*(N_s)$. Implicit in the data collapse in Figure 3b−d is the fact that for $N > N_s$ the relaxation time τ^* for the solvent chains (data not shown) is the same as $\tau^*(N_s)$ for the corresponding pure homopolymer, since the presence of *one* tagged chain of different length should not significantly affect the relaxation dynamics of the solvent chains.

Finally, as an extension of Figure 3d, we show in Figure 4b that when time is scaled by $\tau^*(N_s)f(N/N_s)$, all the underlying

DOI: 10.1021/ma502523p
Macromolecules 2015, 48, 1442−1453

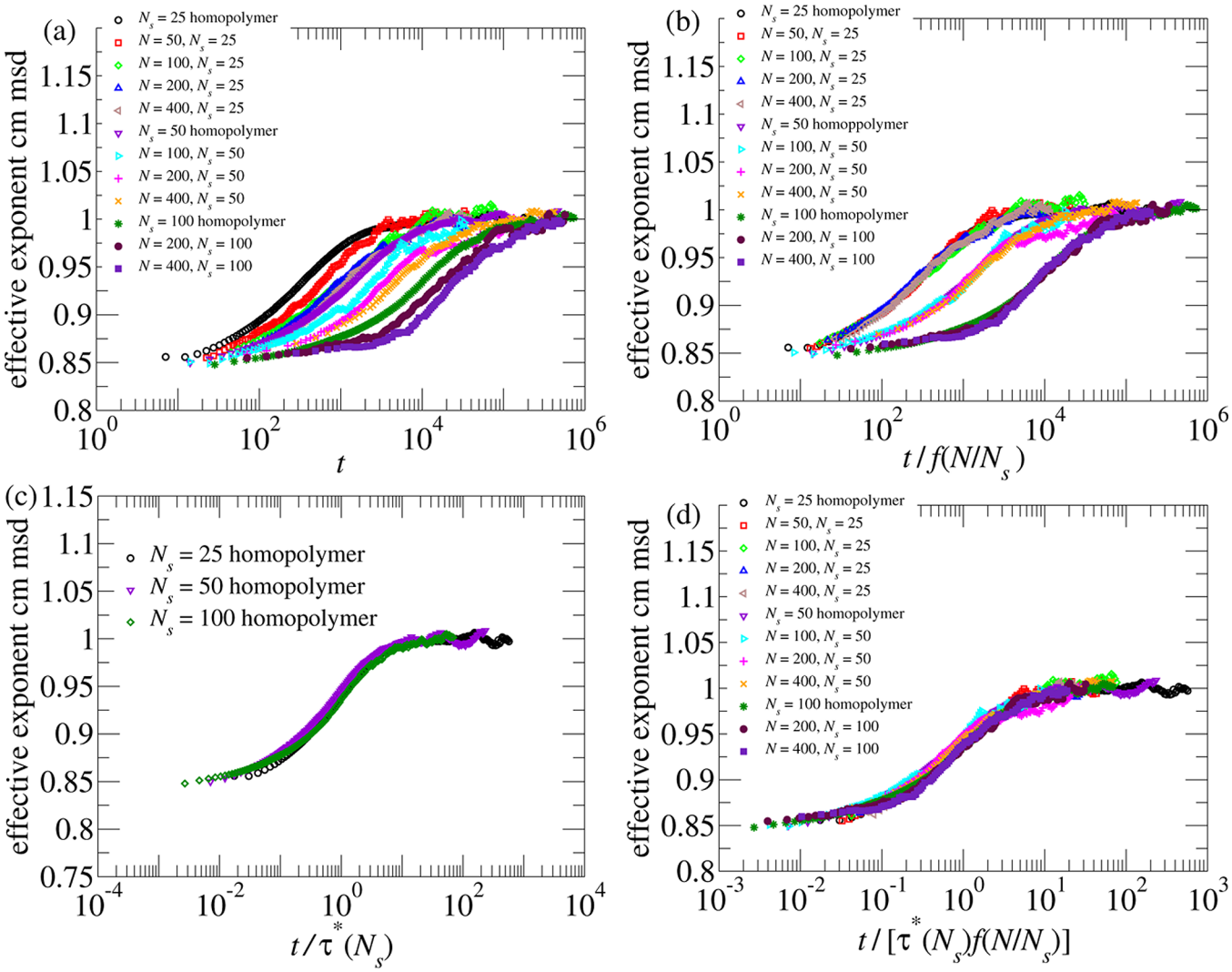

Figure 3. (a) Effective cm msd exponent—numerically differentiated d $\ln(\langle \Delta r_{cm}^2(t) \rangle)$/d $\ln(t)$ data—from our simulations, as a function of t for all our samples corresponding to $N \geq N_s$, showing a crossover from approximately 0.85 to unity. (b) Scaling time by the weakly varying universal scaling function $f(N/N_s)$ given in Table 1 groups the crossover curves according to N_s, showing that it is fundamentally N_s which controls the crossover. (c) For the homopolymer samples, $N = N_s$, scaling time by the characteristic relaxation time scale $\tau^*(N_s)$ for the end-to-end vector correlation, leads to high quality superposition across different N_s. (d) All the cm msd effective exponent data collapse on a single master curve upon rescaling time by $\tau^*(N_s)f(N/N_s)$. See text for details.

Table 1. Values of the Scaling Function $f(N/N_s)$ for All the $N \geq N_s$ Sets[a]

N/N_s	$f(N/N_s)$	(N, N_s) combinations used
1.0	1.0	(25, 25), (50, 50), (100, 100)
2.0	1.7	(50, 25), (100, 50), (200, 100)
4.0	2.6	(100, 25), (200, 50), (400, 100)
8.0	3.1	(200, 25), (400, 50)
16.0	3.4	(400, 25)

[a]Note that the variation is weak, consistent with saturation as N/N_s becomes large.

cm msd curves for the tagged chains collapse on a single master curve. Consequently, the cm msd scales as

$$\langle \Delta r_{cm}^2(t) \rangle \sim \begin{cases} t^{\alpha}/N, & t \leq \tau^*(N_s)f(N/N_s) \\ \{\tau^*(N_s)f(N/N_s)\}^{\alpha-1} t/N, & t > \tau^*(N_s)f(N/N_s) \end{cases} \quad (1)$$

We will see in subsection 2 that the factor $1/N$ in eq 1 can be understood by our blob scaling argument.

The overall conclusion here is that the anomalous diffusion of the chain center of mass is an emergent phenomenon driven by interaction with the solvent chains and controlled by their dynamics. In at least one sense this is not surprising, because we know from earlier work without solvent chains[28] that the dynamics of an isolated single chain in our model yields purely diffusive behavior for the cm msd at *all* times.

2. Scaling Behavior of cm msd: Nature of the Subdiffusion Exponent and Relation to Monomeric Diffusion. Given the long history of the anomalous exponent itself across a wide range of experiments and simulations and debate as to its status, as discussed in our Introduction, it is important to evidence whether the subdiffusion exponent $\alpha \approx 0.85$ we find for the cm msd in our model is a true or an effective exponent. In order to do so, we determine the two-dimensional "exponent flow diagram" in which for an effective exponent such as $\alpha(t) =$ d $\ln\langle \Delta r_{cm}^2(t) \rangle$/d $\ln(t)$ we plot its rate of change with

DOI: 10.1021/ma502523p
Macromolecules 2015, 48, 1442−1453

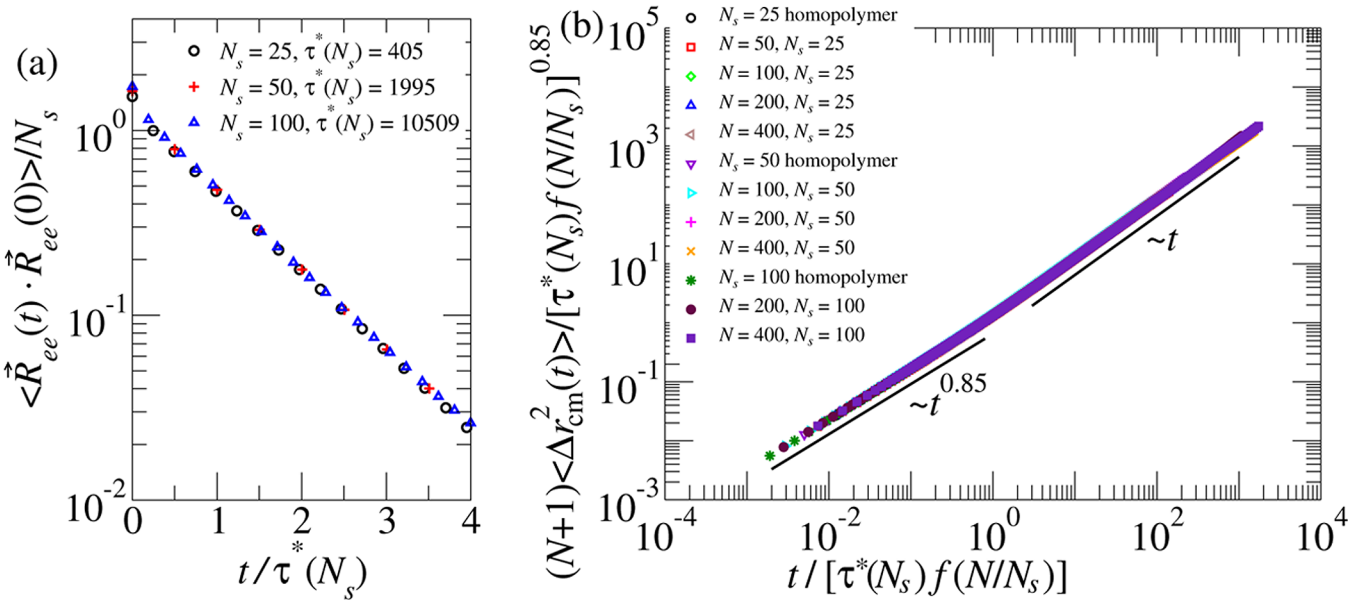

Figure 4. (a) Extracting the (configurational or terminal) relaxation time τ^* of the matrix chains of length N_s. We consider a homopolymer melt of chain length N_s = 25, 50, and 100 and follow the time correlation of the end-to-end vectors of individual chains therein. The data correspond to τ^* = 405, 1995, and 10 509 respectively for N_s = 25, 50, and 100. (b) Data collapse for the cm msd of the tagged chain for all the tagged chain's msd data corresponding to $N \geq N_s$: the master curve shows that for the tagged chain $\langle \Delta r^2_{cm}(t)\rangle \sim t^{0.85}$ until time $\tau^*(N_s)f(N/N_s)$, beyond which the motion of the cm of the tagged chain becomes diffusive.

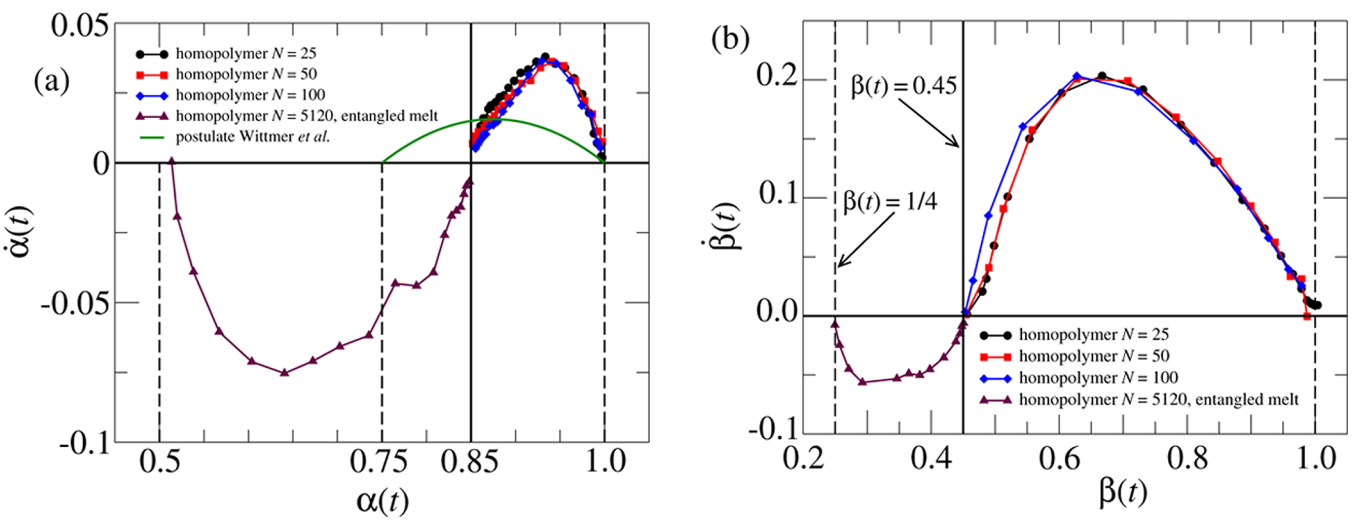

Figure 5. Exponent flow diagrams for unentangled (N = 25, 50, and 100) and entangled (N = 5120) homopolymer melts for the tagged chain's cm (a) and the middle monomer (mm) (b). For the entangled melt, the approach of the effective exponent to 1/2 for the tagged chain cm and 1/4 for the tagged chain mm is clearly consistent with the result of the tube theory due to Doi−Edwards and de Gennes. Importantly, however, they match nicely with the exponents of the unentangled melt at $\alpha \approx 0.85$ and $\beta \approx 0.45$, respectively. Together they demonstrate that these are *true* subdiffusion exponents. Also plotted (a) in solid line is the $\alpha(t)$ vs $\dot{\alpha}(t)$ behavior postulated in refs 7 and 17 which is clearly far from fitting our data (see text for details).

logarithmic time $\dot{\alpha}(t)$ = d $\alpha(t)$/d ln(t) vs the exponent $\alpha(t)$ itself.

In a normalization group picture (if we had one!) the above is equivalent to plotting out the "β-function" (here function g) where $\dot{\alpha} = g(\alpha)$, and we might expect these entire curves to conform within a given universality class. True exponents correspond to fixed points where $\dot{\alpha} = g(\alpha) = 0$. Leading correction to scaling exponents, expressed as $\langle \Delta r^2_{cm}(t)\rangle = At^{\alpha}(1 + Bt^{\delta})$, can also in principle be read off from the slope of $g(\alpha)$ at the fixed points: approaching the fixed point at $\alpha = a$, we have $g'(\alpha) \to \delta$. Positive slope δ corresponds to a fixed point being unstable as $t \to \infty$ and negative slope to stability. A detailed analysis of the values of the exponent δ can be found later in section 3.

We stress that this exercise can only be performed for the homopolymer melts as it requires very high quality data, because computing $\dot{\alpha}$ entails differentiating the (logarithmic) measured mean-squared displacements twice with respect to (logarithmic) time. Acquiring such high quality data for $N \neq N_s$ is prohibitive in practice, restricting this discussion to the homopolymer case. Nevertheless, the advantage of this method is that if the flow diagram crosses the x-axis for a prolonged period of time, then that is a clear indication that the corresponding value of $\alpha(t)$ is a true exponent. Note that there

DOI: 10.1021/ma502523p
Macromolecules 2015, 48, 1442−1453

is precedent for twice differentiating the mean-square displacements: this was previously used in refs 7, 16, and 17 to obtain the velocity autocorrelation function.

We have obtained the exponent flow diagrams for the tagged chain msd for the cm and the middle monomer (mm) for the unentangled (chain lengths 25, 50, and 100) as well as for our recently published data on entangled (chain length 5120) homopolymer melts.[36] These diagrams for the effective exponents $\alpha(t)$ of cm msd and $\beta(t)$ for mm msd are shown in Figure 5. The unentangled chains conform well to a universal curve, and *it should be noted there are no scale factors or fitting parameters behind this agreement*. For the entangled melt, the approach of the effective exponent to 1/2 for the tagged chain cm and 1/4 for the tagged chain mm is clearly consistent with the result of the tube theory due to Doi–Edwards and de Gennes. Most notably, however, the exponent data for the unentangled and entangled melt nicely match with unstable fixed points at $\alpha \approx 0.85$ and $\beta \approx 0.45$, respectively. Figure 5 thus stands as clear evidence of our result that in violation of the Rouse model the cm msd has a *true* subdiffusion exponent approximately 0.85, while the mm msd has a *true* subdiffusion exponent approximately 0.45.

It has been suggested theoretically by others[7,17] that the apparent subdiffusive exponent is simply a result of competing early time behavior, with the cm msd predicted to vary as $at^{3/4} + bt$ for a momentum nonconserving model such as ours. It is easily shown (see Appendix) that the general form $at^p + bt^q$ leads to effective exponent plot $\dot{\alpha} = (\alpha - p)\ (q - \alpha)$. The corresponding predicted curve is shown in Figure 5a for $p = 3/4$ and $q = 1$ and is clearly far from fitting our data. Notably, it is not just a matter of the early time exponent itself but also of the amplitude of the curves: our values of $\dot{\alpha}$ are much higher, meaning that we have a much sharper transition between subdiffusive and diffusive regimes than merely a simple sum of powers, for which $\dot{\alpha}$ peaks too low at $(p - q)^2/4$ and for which the values of $\delta = \pm(p - q)$ are also much too low (see following). Thus, we can conclude that the observed subdiffusive exponent is certainly better modeled as a true exponent than an intermediate between more different powers.

If there is a true renormalization group and scaling underlying this behavior, then we should expect to be able to interpret it in terms of a Pincus–de Gennes dynamical "blob" picture. We assume that over time t the local conformation of the tagged chain is completely reorganized up to a blob scale associated with $g(t)$ monomers[39] and a corresponding spatial length-scale $\xi(t) \propto g(t)^\nu$ which is also the typical distance diffused by individual monomers. We have included a general chain swelling exponent to clarify the argument, but given static screening in the melt the chains should be Gaussian with $\nu = 1/2$. The chain can then be viewed as $N/g(t)$ blobs, each of which has independently displaced by of order $\xi(t) \sim t^{\beta/2}$, where β is the exponent for the mm msd, and the resulting cm motion is given by

$$\Delta r_{\mathrm{cm}}^2(t) \simeq \left\langle \left(\frac{\sum_{\mathrm{blobs}\ b} \delta r_b}{N/g(t)} \right)^2 \right\rangle \simeq \sum_{\mathrm{blobs}\ b} \langle \delta r_b{}^2 \rangle / (N/g(t))^2$$
$$\simeq \xi(t)^2 g(t)/N \propto g(t)^{1+2\nu}/N \propto \xi(t)^{2+1/\nu}/N \qquad (2)$$

where the last relation shows that for Gaussian chains ($\nu = 1/2$) we expect the msd exponents of cm and mm to be related by the scaling law

$$\alpha = 2\beta \qquad (3)$$

This is consistent with our observed values $\alpha \simeq 0.85$ and $\beta \simeq 0.45$. We unify these by taking our *true* subdiffusion exponent to be $\alpha = 2\beta = 0.87 \pm 0.03$ for unentangled melts, which we use throughout the rest of this paper.

Finally we note that the success of this blob argument in inter-relating monomeric and chain center of mass diffusion in our lattice simulations, and further observations discussed further below, is in contrast to the conclusion drawn in ref 14 that their respective departures from Rouse behavior in molecular dynamics simulations have separate origins.

3. Correction to Scaling. The leading correction to scaling exponent for the exponent α near our new subdiffusive fixed point can be immediately understood through the blob picture. If we assume the beads at chain ends are more mobile by a numerical factor (which is exactly two for the Rouse model), then this leads to $\sum_{\mathrm{blobs}\ b} \langle \delta r_b{}^2 \rangle \simeq N/g(t)\xi^2 + a\xi^2$, where a is a positive coefficient of order unity. This then leads to

$$\Delta r_{\mathrm{cm}}^2(t) \simeq \xi(t)^{2+1/\nu}[1 + ag(t)/N]/N$$
$$\simeq \xi(t)^{2+1/\nu}[1 + (a/N)\xi(t)^{1/\nu}]/N \qquad (4)$$

Thus, with leading correction to scaling exponents, expressed earlier as $\langle \Delta r_{\mathrm{cm}}^2(t) \rangle = At^a(1 + Bt^\delta)$, we expect a correction to scaling exponent $\delta = \beta/(2\nu) = \beta \simeq 0.45$ for the cm msd of unentangled chains near the subdiffusive fixed point, and the corresponding slope in 5a is indeed in the range 0.4–0.5.

The corresponding measured value of δ for the exponent β of unentangled chains near the subdiffusive fixed point is at least 2. This fixed point exists even if the melt chains behaved as pure Rouse chains (albeit with $\beta = 1/2$), for which the exponent flow diagram has infinite slope at exponent $\beta = 1/2$, due to corrections to scaling of the form $\exp(-\mathrm{const}/t)$. We suspect that the melt chains in our simulations do retain this property, but our data are by no means conclusive.

Finally, for both α and β near the (stable) diffusive fixed point, the observed correction to scaling exponent is in good agreement with $\delta = -1$. This can be understood rather trivially by the msd (both for cm and mm) behaving as $6Dt + bR_0{}^2 = 6Dt(1 + b'/t)$ for large times, where D is the chain diffusion coefficient, R_0 is a coil radius, and b is a constant of order unity to which constant b' is trivially related.

The way in which the entangled chains exhibit the same subdiffusive fixed point but deviate away from it in opposite direction is further evidence that our subdiffusive regime is a *true* fixed point. If it were simply a short time artifact of the internal chain dynamics, we should expect to see the entangled and unentangled chains deviate from it in the same way at short times, before going their clearly separate ways under the influence of entanglement and finite chain length, respectively. Understanding the correction to scaling exponents on the entangled side of the subdiffusive fixed point requires a model of the early time influence of entanglement. If we follow Edwards[40] in modeling the entanglement tube through a local harmonic potential, then initial calculations indicate that $\delta = 1$ is expected: our data for both α and β are tolerably consistent with this but by no means conclusive.

4. Comparison to Other Non-Momentum-Conserving Models. We now return to discussion of recent work of Wittmer et al.[7] where chains in a melt were allowed to escape entanglement in a different way and which indeed should test our picture above. Specifically, the authors studied bond

DOI: 10.1021/ma502523p
Macromolecules 2015, 48, 1442–1453

fluctuation models, non-momentum conserving like ours, in which chain crossing could occur but only by passing via configurations of overlap incurring significant Boltzmann penalty. The original authors drew attention to how the chains which are (occasionally) allowed to cross through each other exhibit crossover to diffusive motion for the cm. There is a clear parallel with how we see similar crossover brought about by chain ends: in both cases chain crossing is effectively enabled.

While the above study focused on velocity autocorrelation functions, they also published graphs of the cm msd ranging from overlap energy $\varepsilon = 10$, which they showed clearly escapes entanglement, up to $\varepsilon = 100$, which does not. Given that they used second derivatives with respect to time to obtain velocity autocorrelation functions, it is reasonable for us to attempt the same level of differentiation to generate the exponent flow plots. This analysis is shown in Figure 6, and while clearly very

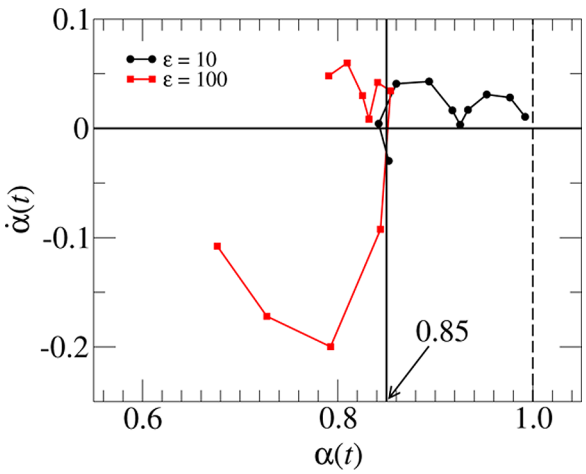

Figure 6. Exponent flow diagrams from the data of Figure 12 in Wittmer et al.[7] corresponding to $N = 8192$.

noisy due to data quality issues, it shows the same trends as our data: there is some approximation to an early time fixed point for α around 0.8−0.85, and then entangled and unentangled chains break away toward their respective entangled and Brownian fixed points. (We do not believe the apparent fixed point around $\alpha = 0.9$ is significant: it is susceptible to the value of one raw data point.) The values of $\dot{\alpha}$ we find from the entangled $\varepsilon = 100$ data run more negative than those we observe from our own $N = 5120$ chains, but given that the BFM models were selected for their rapid onset of entanglement this apparent breach of universality is perhaps not so surprising.

In our picture, the overall implication of the Wittmer et al. results is that it is noncrossing of chains which causes the subdiffusive regime, because as chain crossing becomes allowed the subdiffusive behavior gives way to diffusive motion of the cm. Chain ends then simply have an equivalent effect for otherwise noncrossing chains.

5. Diffusion Coefficient and the Terminal Relaxation Time for the Tagged Chain. Carrying on from our previous subsection A, Figures 3 and 4 distinctly show that the crossover time from subdiffusive to diffusive behavior of the cm msd $\langle \Delta r^2_{\mathrm{cm}}(t)\rangle$ of the tagged chain is given by $\tau^*(N_s)f(N/N_s)$. Matching of the subdiffusive and diffusive regimes for $\langle \Delta r^2_{\mathrm{cm}}(t)\rangle$ at time $\tau^*(N_s)f(N/N_s)$ then yields the diffusion coefficient D of the tagged chain scaling $\sim N^{-1}[\tau^*(N_s)f(N/N_s)]^{\alpha-1}$. For homopolymer melts (of chain length N_s) this not only means $D \sim N_s^{-1}[\tau^*(N_s)]^{\alpha-1}$, but also the scaling of the crossover time $\tau^*(N_s)$ with N_s for homopolymer melts must follow from its correspondence to the terminal relaxation time $\tau^*(N_s)$, since, by time $\tau^*(N_s)$, a tagged chain in a homopolymer melt will have diffused by its own typical size ($\sim\sqrt{N_s}$, with static screening holding true), leading to $D \sim N_s/\tau^*(N_s)$. Comparing the two expressions, we obtain $\tau^*(N_s) \sim N_s^{2/\alpha} = N^{2.30\pm0.08}$, which is very well respected by the values of $\tau^*(N_s)$ reported in Figure 4a.

Furthermore, using the (same) argument that by the terminal relaxation time $\tau_t(N)$ a tagged chain of length N in a matrix of chains of length N_s will have diffused by its own size, we obtain $\tau_t(N) \sim N/D = N^2[\tau^*(N_s)f(N/N_s)]^{1-\alpha}$. In the following subsection we will reinforce this result from the relaxation dynamics of the modes and the mm msd of the tagged chain. In the process doing so we will implicitly confirm that the blob scaling arguments robustly hold for our model.

6. Relaxation Dynamics of the Modes of the Tagged Chain and Its mm msd. We now focus on the structural relaxation aspects of the tagged chain, by considering the mode amplitude autocorrelation function $C_{pq}(t) = \langle \vec{X}_p(t)\cdot\vec{X}_q(0)\rangle$, where $\vec{X}_p(t) \equiv [1/(N+1)]\sum_{n=0}^{N}\cos[(\pi(n+1/2)p)/(N+1)]\vec{R}_n(t)$ is the pth Rouse mode amplitude and $\vec{R}_n(t)$ is the position of the nth monomer at time t. Figure 7a shows the mode amplitude correlation functions for $(p, q) = 1, ..., 4$ and $N = 200$, $N_s = 100$ at four different times. It demonstrates that $C_{pq}(t) \propto \delta_{pq}$; i.e., the modes remain uncorrelated to a very good approximation. Figure 7b then shows that the squared mode amplitude $C_{pp}(0) \sim N/p^2$ (although deviations can be seen higher p/N values, i.e., as shorter length scales), this confirms that the chains in the simulations obey static screening to a good approximation. The most notable point of the structural relaxation of the tagged chain is shown in Figure 7c, where we observe $\chi_{pp}(t) \equiv -\ln[C_{pp}(t)/C_{pp}(0)] \propto (p/N)^2 t^\alpha$ until time $\tau^*(N_s)f(N/N_s)$, again with $\alpha \approx 0.85$, beyond which $\chi_{pp}(t)$ increases linearly in time. Thus, the two configurational relaxation regimes as well as the two dynamical regimes of the cm msd for the tagged chain are consistently separated in time by $\tau^*(N_s)f(N/N_s)$, *a clean signature that the blob scaling arguments in polymer physics holds true for our model.*

Finally, the combined information on the mode amplitudes, their evolution in time, and their orthogonality allows one to derive many other properties analytically.[1] Particularly, the msd of the middle monomer (mm) of the tagged chain is related to the cm msd and the mode amplitudes by

$$\langle \Delta r^2_{\mathrm{mm}}(t)\rangle = \langle \Delta r^2_{cm}(t)\rangle + 8\sum_{p\in\mathrm{even}}[C_{pp}(0) - C_{pp}(t)] \tag{5}$$

Consequently, the mm msd scales as

$$\langle \Delta r^2_{\mathrm{mm}}(t)\rangle \sim \begin{cases} t^{\alpha/2}, & t < \tau^*(N_s)f(N/N_s) \\ [\tau^*(N_s)f(N/N_s)]^{(\alpha-1)/2}t^{1/2}, & \tau^*(N_s)f(N/N_s) \le t \le \tau_t(N) \\ N^{-1}[\tau^*(N_s)f(N/N_s)]^{\alpha-1}t, & t > \tau_t(N) \end{cases} \tag{6}$$

This scaling is verified by the results of direct simulations (Figure 8a,b). Note that in Figure 8a we have used $\alpha/2 = 0.45$, while in Figure 8b we have used $\alpha = 0.85$. As can be seen from eq 1, the two crossovers merge together for homopolymer melts; consequently, the $t^{1/2}$ regime does not exist for them.

Figure 8a also shows that by time $\tau^*(N_s)f(N/N_s)$ the tagged chain's mm displaces itself by $\sim[\tau^*(N_s)f(N/N_s)]^{\alpha/2}$. As

DOI: 10.1021/ma502523p
Macromolecules 2015, 48, 1442−1453

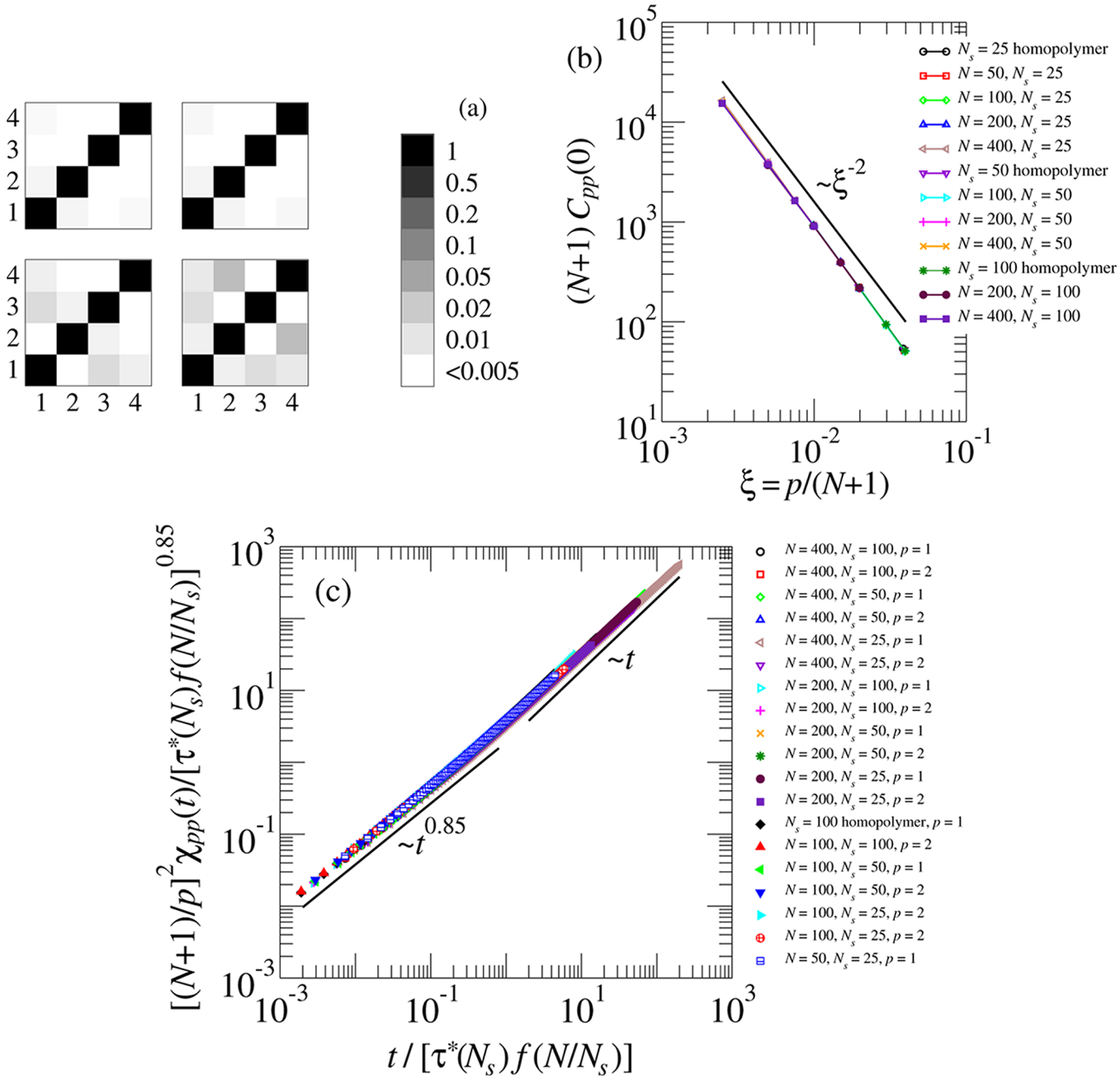

Figure 7. (a) Demonstrating orthogonality of the mode amplitude correlation functions $C_{pq}(t)$, i.e., $C_{pq}(t) \propto \delta_{pq}$ for $(p, q) = 1, ..., 4$, by means of a greyscale checkerboard plot for $N = 200$, $N_s = 100$. Panels: top left $t = 0$, top right $t = 18.2$, bottom left $t = 182$, and bottom right $t = 1820$. Note, from the grayscale bar on the right, that the modes are uncorrelated to a very rather good approximation. (b) Scaling of the squared mode amplitude (zero-time mode correlation function $C_{pp}(0) \sim N/p^2$), demonstrating good agreement with random-walk statistics of the tagged chain, although deviations can be seen for higher p/N values (shorter length scales). (c) Collapse of (19 sets of) normalized mode amplitude correlation function data $\chi_{pp}(t) = -\ln[C_{pp}(t)\ /C_{pp}(0)]$, and the scaling $\chi_{pp}(t) \sim (p/N)^2\ t^{\alpha}$ for $t < \tau*(N_s)$ and $\sim(p/N)^2\{\tau^*(N_s)f(N/N_s)\}^{\alpha-1}t$ for $t > \tau^*(N_s)$.

discussed in subsection 5, $\tau^*(N_s)^{2/\alpha} \sim R_s$. Since the value of the scaling function $f(N/N_s)$ is of order unity, Figure 8a then implies that by time $\tau^*(N_s)f(N/N_s)$ the tagged chain's monomers displace themselves by a distance that is of the order of the typical size of the matrix chains.

B. Case $N \leq N_s$. Next we consider the case $N \leq N_s$. Taking the cue from homopolymer results, we expect the subdiffusive regime for the cm msd of the tagged chains to last all the way to their terminal relaxation time $\tau_t(N)$. We also expect to find $\tau_t(N) = \tau^*(N)f(N_s/N)$ for some scaling function f, where $\tau^*(N)$ is identified from the corresponding homopolymer samples of length N, as we have done in Figure 4a. Interestingly, for the $N \leq N_s$ combinations we have chosen, we find that the values of $f(N_s/N)$ can simply be read off from Table 1, although there is *a priori* no reason for this to hold.

Our data confirming the above are plotted in Figure 9. Figure 9a shows the collapse of the cm msd data: $\langle \Delta r^2_{cm}(t)\rangle \sim t^{\alpha}$, with $\alpha \approx 0.85$ until time $\tau_t(N) = \tau^*(N)f(N_s/N)$, after which the motion of the cm is diffusive, with a diffusion coefficient D scaling $\sim N^{-1}[\tau^*(N)f(N_s/N)]^{\alpha-1}$. Figure 3b shows that the normalized mode amplitude autocorrelation functions decay as stretched exponentials in time, with the same exponent α until

DOI: 10.1021/ma502523p
Macromolecules 2015, 48, 1442−1453

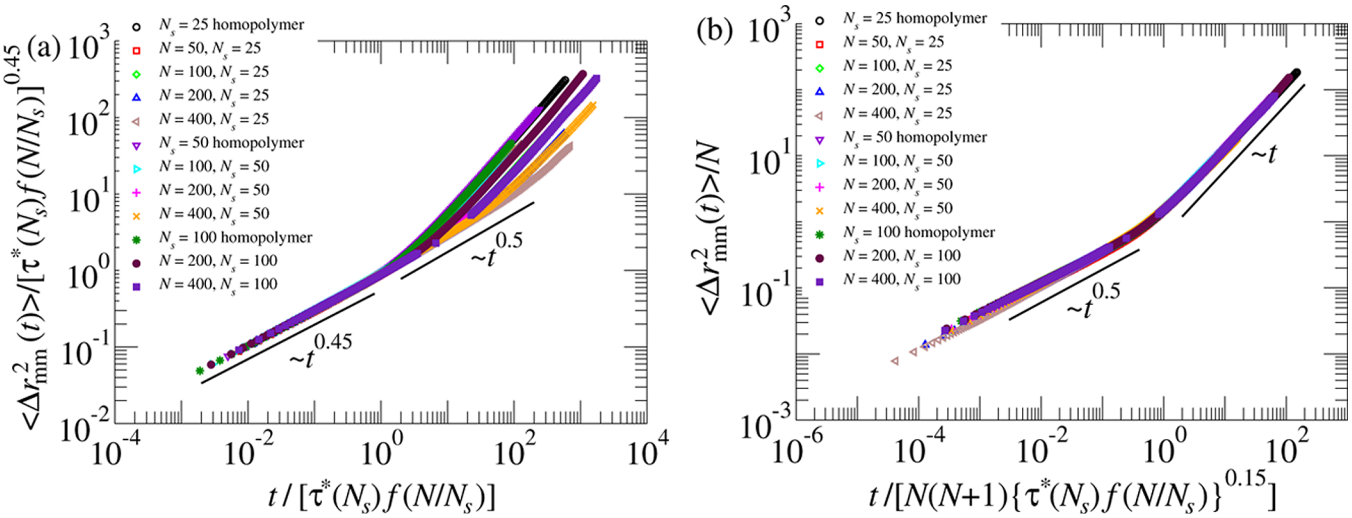

Figure 8. Data collapse of the mm msd for the tagged chain. For $N > N_s$ the mm msd has two crossovers: at $\tau^*(N_s)f(N/N_s)$ and at $\tau_t(N_s) \sim N^2[\tau^*(N_s)f(N/N_s)]^{1-\alpha}$. Part (a) brings together the first crossover: for $t < \tau^*(N_s)$, the mm msd scales $\sim t^{\alpha/2}$, while for $\tau^*(N_s)f(N/N_s) < t < \tau_t(N_s)$ the mm msd scales $\sim t^{1/2}$. Part (b) brings together the second crossover: for $t < \tau_t$ the motion of the mm is diffusive with diffusion coefficient $D \sim N^{-1}[\tau^*(N_s)f(N/N_s)]^{\alpha-1}$, determined in subsection 5 from the cm msd data, as it should be. Note that in part (a) we have used $\alpha/2 = 0.45$, while in part (b) we have used $\alpha = 0.85$. For homopolymer melts the two crossovers merge into one; consequently, the $t^{1/2}$ regime does not exist for them.

$\tau_t(N)$, and exponentially thereafter. The mm is also subdiffusive until τ_t and diffusive thereafter; once again, for the subdiffusive part we have used $\alpha/2 \approx 0.45$.

C. Summary of the Main Results. Taken together, the data of subsections A and B thus yield two *true* exponents: $\alpha = 0.87 \pm 0.03$ and $\beta = \alpha/2$. Correspondingly, the scalings of the tagged chain's terminal relaxation time $\tau_t(N)$ and its diffusion coefficient D are shown in Table 2.

IV. COMPARISON WITH EXPERIMENTS

We believe that in the end experiments will have to settle the value of the anomalous exponent α. In this context we note that there is evidence from experimental literature[9,10] that the autocorrelation function between the Rouse mode amplitudes decays as stretched exponentials.

A. Neutron Spin Echo and Dynamic Rheology. The "anomalous" time scaling results obtained by our lattice Monte Carlo simulation results is also consistent with experiments. Experimentally, the most direct probe of monomeric diffusion comes from time-dependent incoherent scattering probed by neutron spin echo.[41] These measurements were noted to be consistent with Rouse monomeric msd, but we find that a free fit to the power law regime favors $\alpha/2 \simeq 0.44$, albeit the Rouse value 1/2 cited by the original authors is not excluded.

The blob argument enables us to also relate to dynamical rheology experiments where again we find agreement. For the dynamic rheology we consider the stress response time t after the application of an imposed step strain: assuming that the associated modulus should be k_BT per blob, this leads to $G(t) \simeq ck_BT/g(t)$, where c is the monomer concentration. The corresponding prediction for the frequency-dependent storage modulus is then $G(\omega) \propto (\omega)^{\alpha/2}$, which is shown in Figure 10 to agree with relatively recent experiments on unentangled homopolymer melts by Majeste et al.,[22] who also commented on the dearth of earlier clean data in the unentangled regime.

The corresponding homopolymer melt viscosity scaling $\eta \sim \tau_t/N \propto N^{2/\alpha-1} = N^{1.30\pm0.08}$ and $D \sim N^{1-2/\alpha} = N^{-(1.30\pm0.08)}$ are more difficult to check experimentally, because one must correct for the molecular weight dependence of the local monomeric friction factor.[42] A number of authors have over the years confirmed that at constant friction factor, unentangled melts have $\eta \propto N^\beta$ with exponent β closer to 1.2 than the Rouse value of unity, albeit not as large as the value $\beta = 1.32$ implied by $\alpha = 0.86$. Williams[43] first reported $\beta = 1.12$; Majeste et al. found $\beta = 1.25$ for polystyrene[22] and cited Pearson's careful study of alkanes[44] yielding $\beta = 1.17$. For many years the discrepancy from the Rouse scaling of viscosity was attributed to possible (but not measured) variation[45] of the ratio $R^2(N)/N$: both the Rouse model and our blob generalization above share the property that $\eta D \simeq R^2(N)/N$. However, this was found to be impressively constant by Pearson for unentangled alkanes[44] and PEB2 and polystyrene:[46] in the latter case it was also noted that actual melt based measurements of $R^2(N)/N$ were too constant over the mass range of interest to bring the value of β sufficiently close to the Rouse value of unity.

More recently, Meier et al.[47] have attempted to directly separate the dependence of D on N and local segment mobility, across a wide range of polymers. They comment that "pure Rouse behavior is difficult to identify", and above a rather low crossover mass (which for PDMS is around $M_e/6$) they show D varying more steeply with N than in the Rouse model—albeit not with particularly uniform exponent.

B. NMR Relaxometry. A variety of NMR techniques[23−26,48,49] give direct measurement of the tensorial segmental orientation autocorrelation function

$$C(t) = \left\langle \frac{(3b_z(t+\tau)^2 - b^2)}{2b^2} \frac{(3b_z(\tau)^2 - b^2)}{2b^2} \right\rangle_{\tau,\text{ensemble}}$$

as a function of time lag t, where the local bond vector has component $b_z(t)$ along the NMR field axis and fixed length b. For lag t exceeding single segment time scales we can express $b_z(t)$ as the sum of a contribution from the coarser grained chain configuration $(\delta z/\delta n)(t)$ plus contributions from local isotropic fluctuations, where $z(n)$ is the projection of the chain configuration along the NMR field (as a function of monomer index n). If we assume the $(\delta z/\delta n)(t)$ are approximately joint Gaussian distributed, or equivalently neglect fourth-order

DOI: 10.1021/ma502523p
Macromolecules 2015, 48, 1442−1453

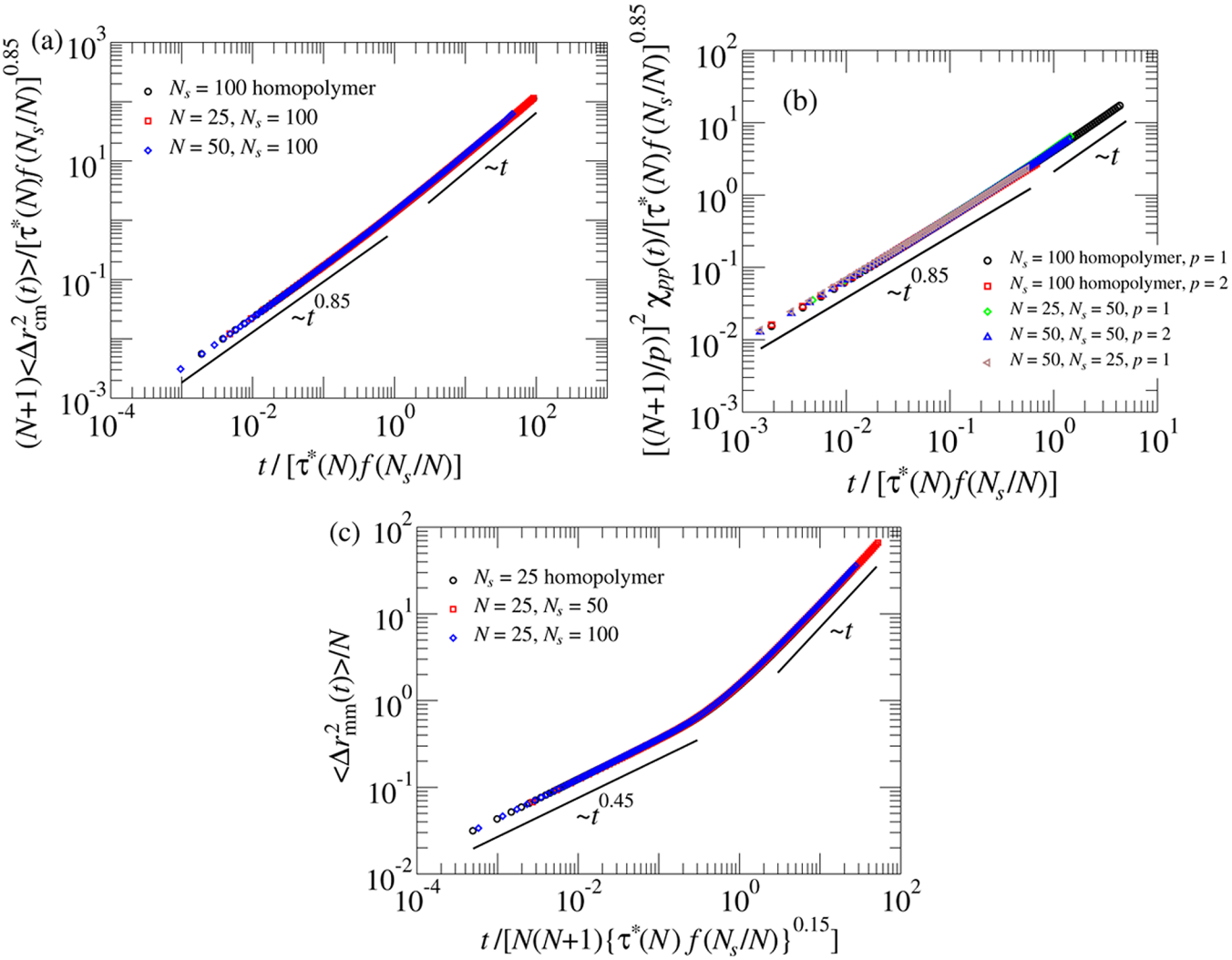

Figure 9. Scaling collapse of the cm msd, mode amplitudes and mm msd data for the tagged chain for $N < N_s$. (a) $\langle \Delta r_{mm}{}^2(t)\rangle \sim t^{\alpha}$, with $\alpha \approx 0.85$ until time $\tau_t(N) = \tau^*(N)f(N_s/N)$, after which the motion of the cm is diffusive. (b) Collapse of 5 sets of normalized mode amplitude correlation function data $\chi_{pp}(t) = -\ln[C_{pp}(t)/C_{pp}(0)]$ and the scaling $\chi_{pp}(t) = (p/N)^2 t^{\alpha}$ until time $\tau_t(N)$, beyond which $\chi_{pp}(t) = (p/N)^2\{\tau^*(N)f(N_s/N)\}^{\alpha-1}t$ and $\alpha \approx 0.85$. (c) $\langle \Delta r_{mm}{}^2(t)\rangle \sim t^{\alpha/2}$ until time $\tau_t(N)$, after which the motion of the mm is diffusive; once again, for the subdiffusive part we have used $\alpha/2 \approx 0.45$.

Table 2. Scalings of the Tagged Chain's Terminal Relaxation Time $\tau_t(N)$ and Its Diffusion Coefficient D

	$N \geq N_s$	$N \leq N_s$
D	$\sim N^{-1}[\tau^*(N_s)f(N/N_s)]^{\alpha-1}$	$\sim N^{-1}[\tau^*(N)f(N_s/N)]^{\alpha-1}$
$\tau_t(N)$	$\sim N^2[\tau^*(N_s)f(N/N_s)]^{1-\alpha}$	$\sim \tau^*(N)f(N_s/N)$

cumulant contributions, then the above displayed expression reduces to

$$C(t) = 9/2\left\langle \frac{\delta z}{\delta n}(t+\tau)\frac{\delta z}{\delta n}(\tau)/b^2\right\rangle^2_{\tau,\text{ensemble}}$$

One can apply an equivalent analysis to the dipolar autocorrelation function

$$C_d(t) = 3\langle b_z(t+\tau)b_z(\tau)/b^2\rangle_{\tau,\text{ensemble}}$$

leading to the identification

$$C(t) = (1/2)C_d(t)^2$$

for lag t greater than single segment time scales. A similar result is also obtained in ref 50. *Note that this result only holds in the pre-entangled regime.*

The autocorrelation functions are now both readily predicted in terms of the blob scaling. We coarse grain up to the scale of blobs unrelaxed in time t to obtain $b_z \simeq \delta z/\delta n \simeq \xi(t)/g(t)$, and hence $C_d(t) \simeq [\xi(t)/g(t)]^2 \propto \xi(t)^{2-2/\nu}$. For Gaussian chains this then gives $C_d(t) \propto \xi(t)^{-2} \propto t^{-\alpha/2}$, and correspondingly $C(t) \propto t^{-\alpha}$. This last result can also be obtained directly from blob arguments rather than via C_d. The corresponding data obtained from our lattice model have been presented in Figure 8 of our recently published paper[36] for entangled melt in the pre-entangled regime, showing $C(t) \sim t^{-0.83\pm0.01}$. This is in excellent agreement with the experimental observation $C(t) \sim t^{-0.85}$ obtained from T1 relaxometry data.[24] We should note here that proton T_1 relaxometry does not only probe the tensorial segmental orientation correlation function but also the intermolecular correlation function (dominated by translational motion) and thus cannot easily discriminate between the two contributions. Yet, applying isotope dilution experiments, in the regime of the Rouse dynamics the influence of the

DOI: 10.1021/ma502523p
Macromolecules 2015, 48, 1442−1453

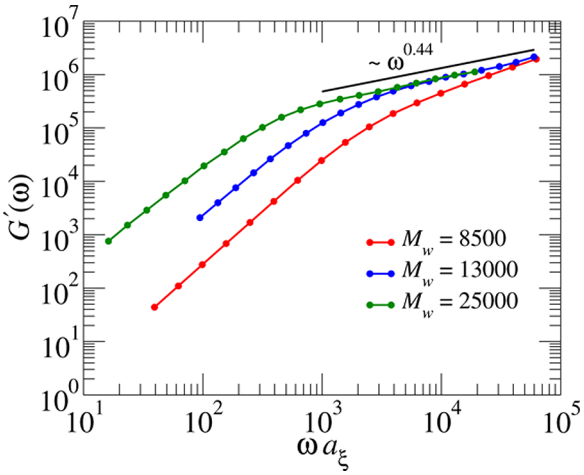

Figure 10. Dynamic storage modulus $G'(\omega)$ vs ω measurements by Majeste et al.[22] for three polystyrene samples of intermediate molecular weight as indicated, where the frequency axis has been shifted to constant monomeric friction factor a_ξ according to the classical "WLF" methodology described in ref 42, using the WLF parameters.[22] There is a clear common scaling region compatible with $G'(\omega) \propto \omega^{0.44}$.

intermolecular relaxation turns out to be ignorable,[26] and indeed there the exponents agree with our reported value of α. Recent independent measurement of $C(t)$ using multiple quantum-proton NMR by the Saalwächter group[51] reinforcing the $C(t)$ exponent in the range ≈0.8 lends further credibility to experimental confirmation of our reported exponent α.

V. CONCLUSION

To conclude, our simulations clearly show that the subdiffusion exponent $\alpha = 0.87 \pm 0.03$ for the tagged chain's cm motion is an effect of the surrounding chains, as evidenced by the dependence of its crossover time to Fickian diffusion on their molecular weight for $N_s > N$. Moreover, the internal chain motions for the polymer's modes and the middle monomer scale correspondingly differently from the Rouse model.

The anomalous scaling we observe extends over more than 3 orders of magnitude in time. However, ultimately this range is limited by the finite range of molecular weight between the onset of coil overlap and the onset of entanglement—typically a ratio approaching 100 leading to a ratio in time of order 10^4, consistent with what we observe. It follows that, given only this finite range, we cannot identify a true (for example asymptotic) power law through observing just one log−log plot: preference for a power law has to rest on the coherence and simplicity of the overall picture.

Our measured exponent flow diagrams however provides key support for the observed subdiffusive value of α being a true "fixed point" exponent, rather than the influence of a correction to Rouse scaling. This in turn supports a blob model of the local scaling which successfully relates other observed exponents, including evidence from dynamical rheology for unentangled homopolymer melts. Such scaling arguments suggest correspondingly anomalous scaling of viscosity and self-diffusion coefficient with molecular weight, seen in classical experiments on unentangled homopolymer melts (albeit to a lesser extent).

We can offer a hint at understanding the value of α by noting that the Rouse model assumes that the motion of one chain is accommodated without large scale displacement of surrounding ones, which our observed N_s dependence of the time scales shows is not correct. If instead we assume the displacement of a blob of $g(t)$ monomers entrains comparable displacement of all the monomers within a blob radius $\xi(t) \simeq g(t)^{1/2}$, where we have used Gaussian chain statistics, but we still use screened hydrodynamics,[3] then we expect the drag coefficient for the blob to scale proportional to its mass $\xi(t)^3$ and hence $d[\xi(t)^2]/dt \propto \xi(t)^{-3}$, leading to $g(t) \propto t^{2/5}$. Thus, this "screened entrainment" argument leads to $\alpha = 4/5$, not so far from the observed values.

The entrained blob picture also provides a simple interpretation of the crossover to Fickian behavior of the cm set by the solvent chains. The velocity fluctuations of the solvent chain fluid are not expected to show more than minimal hydrodynamic consistency for length scales and time scales exceeding the solvent chain size and relaxation time. By the fluctuation−dissipation theorem there is a corresponding falloff in the hydrodynamic propagator giving the velocity response to an applied force. If we then model a tagged chain as applying entropic forces to the surrounding solvent chains, the response is predominantly localized within of order the solvent chain dimensions, and for larger length and time scales of tagged chain motion a renormalized Rouse model results.

Within this view it seems most revealing that earlier simulation studies allowing chain crossing also exhibit crossover from subdiffusive to Fickian behavior. The dilemma we then face is to separate the dynamical constraint of noncrossing from the more severe and quasi-equilibrium constraint of full blown entanglement. We speculate that this relates to the separate continuity of velocity field (hence strain) and of stress field, whose combination underpins bulk rheology. Noncrossing is certainly key to the anomalous subdiffusion we observe and is also key to the existence of unambiguous velocity field at the monomeric level: thus we propose to associate subdiffusion with continuity of the dynamical velocity field. This would leave full blown entanglement to be associated with continuity of the stress field which is a quasi-equilibrium property.

Taken together, our results imply that there is more to the scaling of unentangled melts than the Rouse model which has dominated the field for half a century, but a full and consistent theory of the anomaly has yet to be found. We are now in the process of studying unentangled polymer melts using momentum-conserving models such as the Kremer−Grest model, and the results will appear in a future publication.

■ APPENDIX. $\dot{\alpha}$ vs α CURVE FOR A CROSSOVER FROM 3/4 TO 1

In this appendix we provide the relation between $\dot{\alpha}$ and α for the cm msd as postulated by Wittmer et al.,[7] namely that $\langle \Delta r_{cm}^2(t) \rangle = at^p + bt^q$, with two constants a and b. We show that the $\dot{\alpha}$ vs α curve is independent of the two constants a and b.

For brevity of notations we write

$$\ln y(t) = \ln\langle \Delta r_{cm}^2(t) \rangle = \ln a + p \ln t + \ln[1 + Be^{(q-p)\ln t}] = \ln a + px + \ln[1 + Be^{(q-p)x}] \tag{A1}$$

where $B = b/a$ and $x = \ln t$. This implies that

DOI: 10.1021/ma502523p
Macromolecules 2015, 48, 1442−1453

$$\alpha(t) = \frac{\mathrm{d}\ln y(t)}{\mathrm{d}\ln t} = p + (q-p)\frac{Be^{(q-p)x}}{[1 + Be^{(q-p)x}]} = q - \frac{q-p}{[1 + Be^{(q-p)x}]} \tag{A2}$$

i.e.

$$1 + Be^{(q-p)x} = \frac{q-p}{q-\alpha(t)} \tag{A3}$$

Using eq A2 and the definition of $\dot{\alpha}(t)$, we obtain

$$\dot{\alpha}(t) = \frac{\mathrm{d}\alpha(t)}{\mathrm{d}x} = \frac{B(q-p)^2 e^{(q-p)x}}{[1 + Be^{(q-p)x}]^2} = \frac{(q-p)^2}{[1 + Be^{(q-p)x}]} \times \left[1 - \frac{1}{1 + Be^{(q-p)x}}\right] = (q-p)[q-\alpha(t)] \times \left[1 - \frac{\{q-\alpha(t)\}}{q-p}\right] = -[p-\alpha(t)][q-\alpha(t)] \tag{A4}$$

which is then plotted in Figure 5a in solid lines for $p = 3/4$ and $q = 1$. Also, note from eq A4 that $\dot{\alpha}(t)$ peaks at $(p-q)^2/4$.

AUTHOR INFORMATION

Corresponding Author

*E-mail d.panja@uu.nl (D.P.).

Notes

The authors declare no competing financial interest.

ACKNOWLEDGMENTS

We gratefully acknowledge J.-C. Majeste for readily sharing his experimental data, which have been used in Figure 10. R.C.B. acknowledges support from the UK Engineering and Physical Sciences Research Council grant EP/I01358X/1.

REFERENCES

(1) Doi, M.; Edwards, S. F. *The Theory of Polymer Dynamics*, revised ed.; Clarendon Press: Oxford, 2003.
(2) Rouse, P. E. *J. Chem. Phys.* **1953**, *21*, 1272−1280.
(3) Freed, K. F.; Edwards, S. F. *J. Chem. Phys.* **1974**, *61*, 3626−3633.
(4) Shaffer, J. S. *J. Chem. Phys.* **1995**, *103*, 761−772.
(5) Paul, W.; Binder, K.; Heermann, D.; Kremer, K. *J. Chem. Phys.* **1999**, *95*, 7726−7740.
(6) Padding, J. T.; Briels, W. J. *J. Chem. Phys.* **2002**, *117*, 925−943.
(7) Wittmer, J. P.; Polińska, P.; Meyer, H.; Farago, J.; Johner, A.; Baschnagel, J.; Cavallo, A. *J. Chem. Phys.* **2011**, *134*, 234901.
(8) Paul, W.; Smith, G. D. *Rep. Prog. Phys.* **2004**, *67*, 1117−1185.
(9) Paul, W.; Smith, G. D.; Yoon, D. Y.; Farago, B.; Rathgeber, S.; A.Zirkel, A.; Willner, L.; Richter, D. *Phys. Rev. Lett.* **1998**, *80*, 2346−2349.
(10) Pérez-Aparicio, R.; Alvarez, F.; Arbe, A.; Willner, L.; Richter, D.; Falus, P.; Colmenero, J. *Macromolecules* **2011**, *44*, 3129−3139.
(11) Schweizer, K. S. *J. Chem. Phys.* **1989**, *91*, 5802−5821.
(12) Fatkullin, N. F.; Kimmich, R.; Kroutieva, M. *J. Exp. Theor. Phys.* **2000**, *91*, 150−166.
(13) Guenza, M. *J. Chem. Phys.* **1999**, *110*, 7574−7588.
(14) Guenza, M. *Phys. Rev. Lett.* **2002**, *88*, 025901.
(15) Zamponi, M.; Wischnewski, A.; Monkenbusch, M.; Willner, L.; Richter, D.; Falus, P.; Farago, B.; Guenza, M. G. *J. Phys. Chem. B* **2008**, *112*, 16220−16229.
(16) Farago, J.; Meyer, H.; Baschnagel, J.; Semenov, A. N. *Phys. Rev. E* **2012**, *85*, 051806.
(17) Farago, J.; Meyer, H.; Baschnagel, J.; Semenov, A. N. *Phys. Rev. E* **2012**, *85*, 051807.
(18) Smith, B. A.; Samulski, E. T.; Yu, L.-P.; Winnik, M. A. *Phys. Rev. Lett.* **1984**, *52*, 45−48.
(19) Smith, B. A.; Samulski, E. T.; Yu, L.-P.; Winnik, M. A. *Macromolecules* **1985**, *18*, 1901−1905.
(20) Green, P.; Kramer, E. J. *Macromolecules* **1986**, *19*, 1108−1116.
(21) Ball, R. C.; Callaghan, P. T.; Samulski, E. T. *J. Chem. Phys.* **1997**, *106*, 7352−7361.
(22) Majeste, J. C.; Montfort, J.-P.; Allal, A.; Marin, G. *Rheol. Acta* **1998**, *37*, 486−499.
(23) Kariyo, S.; Gainaru, C.; Schick, H.; Brodin, A.; Novikov, V. N.; Rössler, E. A. *Phys. Rev. Lett.* **2006**, *97*, 207803.
(24) Herrmann, A.; Novikov, V. N.; Rössler, E. A. *Macromolecules* **2009**, *42*, 2063−2068.
(25) Herrmann, A.; Kresse, B.; Gmeiner, J.; Privalov, A. F.; Kruk, D.; Fujara, F.; Rössler, E. A. *Macromolecules* **2012**, *45*, 1408−1416.
(26) Hofmann, M.; Herrmann, A.; Abou Elfadl, A.; Kruk, D.; Wohlfahrt, M.; Rössler, E. A. *Macromolecules* **2012**, *45*, 2390−2401.
(27) van Heukelum, A.; Barkema, G. T. *J. Chem. Phys.* **2003**, *119*, 8197−8202.
(28) Panja, D.; Barkema, G. T. *J. Chem. Phys.* **2009**, *131*, 154903.
(29) Carmesin, I.; Kremer, K. *Macromolecules* **1988**, *21*, 2819−2823.
(30) Klein Wolterink, J.; Barkema, G. T.; Cohen Stuart, M. A. *Macromolecules* **2005**, *38*, 2009−2014.
(31) Klein Wolterink, J.; Barkema, G. T.; Panja, D. *Phys. Rev. Lett.* **2006**, *96*, 208301.
(32) Panja, D.; Barkema, G. T.; Ball, R. C. *J. Phys.: Condens. Matter* **2007**, *19*, 432202.
(33) Vocks, H.; Panja, D.; Barkema, G. T.; Ball, R. C. *J. Phys.: Condens. Matter* **2008**, *20*, 095224.
(34) Panja, D.; Barkema, G. T. *Biophys. J.* **2008**, *94*, 1630−1637.
(35) Panja, D.; Barkema, D. G. T.; Kolomeisky, A. B. *J. Phys.: Condens. Matter* **2009**, *21*, 242101.
(36) Furtado, F.; Damron, J.; Trutschel, M.-L.; Franz, C.; Klaus Schröter, R. C.; Ball, K.; Saalwächter; Panja, D. *Macromolecules* **2014**, *47*, 256−268.
(37) Walter, J.-C.; Baiesi, M.; Carlon, E.; Schiessel, H. *Macromolecules* **2014**, *47*, 4840−4846.
(38) Baiesi, M.; Carlon, E. *Markov Processes Relat. Fields* **2013**, *19*, 569−576.
(39) de Gennes, P.-G. *Scaling Concepts in Polymer Physics*, revised ed.; Cornell University Press: Ithaca, NY, 1985.
(40) Edwards, S. F. *Proc. Phys. Soc. London* **1967**, *92*, 9−16.
(41) Wischnewski, A.; Monkenbusch, M.; Willner, L.; Richter, D. *Phys. Rev. Lett.* **2003**, *90*, 058302.
(42) Williams, M. L.; Landel, R. F.; Ferry, J. D. *J. Am. Chem. Soc.* **1955**, *77*, 3701−3707.
(43) Williams, M. L. *J. Appl. Phys.* **1958**, *29*, 1395−1398.
(44) Pearson, D. S.; Ver Strate, G.; von Meerwall, E.; Schilling, F. C. *Macromolecules* **1987**, *20*, 1133−1141.
(45) Berry, G. C.; Fox, T. G. *Adv. Polym. Sci.* **1968**, *5*, 261−357.
(46) Pearson, D. S.; Fetters, L.; Graessley, W. W.; Ver Strate, G.; von Meerwall, E. *Macromolecules* **1994**, *27*, 711−719.
(47) Meier, R.; Herrmann, A.; Hofmann, M.; Schmidtke, B.; Kresse, B.; Privalov, A. F.; Kruk, D.; Fujara, F.; Rössler, E. A. *Macromolecules* **2013**, *46*, 5538−5548.
(48) Graf, R.; Heuer, A.; Spiess, H. W. *Phys. Rev. Lett.* **1998**, *80*, 5738−5741.
(49) Saalwächter, K. *Prog. NMR Spectrosc.* **2007**, *51*, 1−35.
(50) Wang, Z.; Likhtman, A. E.; Larson, R. G. *Macromolecules* **2012**, *45*, 3557−3570.
(51) Saalwächter, K., private communication.

DOI: 10.1021/ma502523p
Macromolecules 2015, 48, 1442−1453